MŰEGYETEM 1782

AXIALLY LOADED FRP CONFINED REINFORCED CONCRETE CROSS-SECTIONS

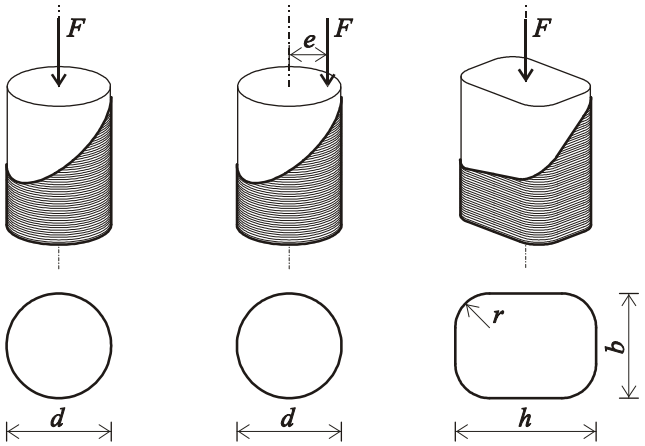

Bernát Csuka

Budapest University of Technology and Economics
Department of Mechanics Materials and Structures

Supervisor: László P. Kollár

1. INTRODUCTION

Axial resistance of concrete and reinforced concrete columns can be significantly increased by using lateral confinement. Frequently used solutions are steel helices, jackets or tubes.

In the last 20 years – instead of steel jackets – the use of FRP (fiber reinforced polimer) as confinement has increased due to its high corrosion resistance, high ultimate stress and because it is easy to use for repair and/or reinforcement of damaged columns. FRP confinement can be applied to any type of cross-sections but most frequently circular- and rectangular cross-sections (with rounded edges) are used.

Due to the loads internal forces develop in the column, which may result in failure. The internal forces are:

- axial force (due to concentric axial load Figure 1.1a),
- axial force and bending moment (due to eccentric axial – or axial and horizontal – load Figure 1.1b) and
- shear force (due to horizontal load Figure 1.1c – horizontal load also causes bending moment).

In this thesis only the first two are investigated.

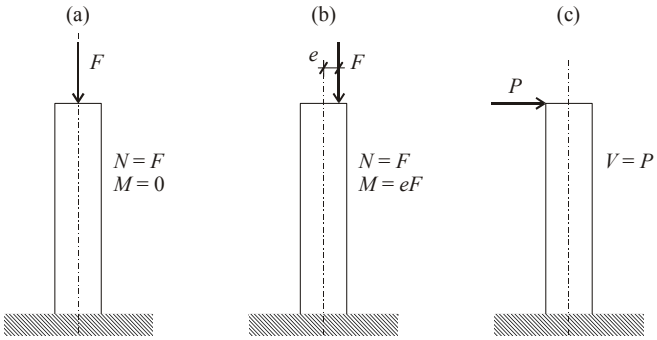

Figure 1: Typical loads on a column: concentric compression (a), eccentric compression (b) and horizontal load (c).

Behavior of confined materials: The concrete core of an axially loaded column laterally expands due to the Poisson-effect. The confinement hinders this expansion and hence the concrete is subjected to triaxial compression and its axial resistance increases.

The confining stress σ_l in case of circular cross-sections can be calculated as follows (Figure 2):

$$\sigma_l = \frac{2\sigma_f t}{d}, \tag{1}$$

where σ_f is the hoop stress in the confinement; t is the thickness of the confinement and d is the diameter of the cross-section.

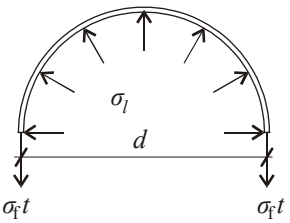

Figure 2: Confined circular cross-section.

The behavior of confined materials has already been investigated for 100. Kármán [3] experimentally investigated rigid materials (marble and sandstone) in triaxial stress-state and found that with proper confinement plastic or even hardening behavior can be achieved.

1.1 Concentrically loaded circular cross-sections

There are several experimental results and models for *concentrically loaded* FRP confined *circular* columns. Models are based either on experimental data (design oriented models) or on triaxial concrete material models (analysis oriented models).

According to the models the failure strength of FRP confined column is not affected by the stiffness of the confinement. We may observe, however, that for a very soft confinement the concrete might fail before the development of the confining stresses, and for a very rigid FRP the confinement may fail before the concrete reaches its plastic state.

1.2 Eccentrically loaded circular cross-sections

Relatively few documented experiments on *eccentrically loaded* FRP confined *circular* columns can be found in the literature. There are two types of models: simplified models [1,2], where the Bernaulli-Navier hypothesis (plane cross-sections remain plane) is combined with an axial stress-strain curve of concrete for concentric loading [4] (which contains the effect of confinement); and numerical 3D models, using commercially available FE programs with built-in triaxial material model for concrete.

Existing simplified models fail to properly predict the behavior of eccentrically loaded confined columns (Figure 3) while in numerical models only qualitative comparisons with experiments were made. Authors also admit [1] that “further research in this area is needed”.

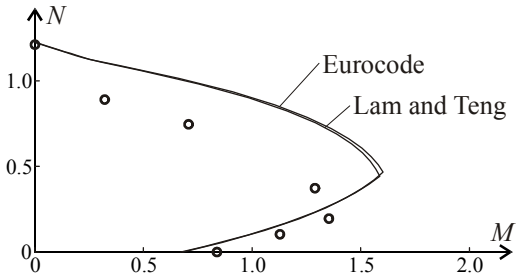

Figure 3: Comparison of experimental results and simplified models.

1.3 Concentrically loaded rectangular cross-sections

For *concentrically loaded* FRP confined *rectangular* columns (with rounded edges) numerous experimental results are available in the literature. There are simplified models based on design-oriented models for concentrically loaded circular columns using different methods to find an "equivalent diameter" and effective area; and numerical 3D models similar to those used for eccentrically loaded circular columns.

For the numerical models again only quantitative comparisons with experiments were made; while no simplified model is available in the literature which can predict reliably the experimental data. This can be observed very clearly in Figure 4, where the data is given as a function of the relative corner radius.

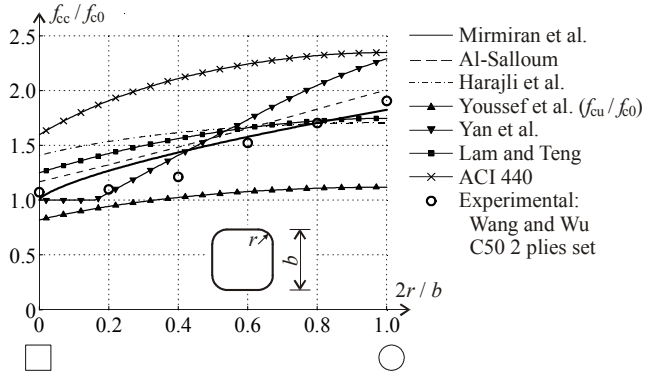

Figure 4: Effect of rounding of the edges on the ratio of confined strength (f_{cc}) to unconfined strength (f_{c0}) for square sections.

2. PROBLEM STATEMENT

Based on the information found in the literature the following questions arise for *concentrically loaded* FRP confined *circular* columns:

- How does the stiffness of FRP confinement affect the behavior of the confined concrete column?
- Under what conditions can it be assumed, that the strength of the confined concrete is not affected by the stiffness of the confinement?

These questions have practical importance as the stiffness of FRP may strongly vary and, in addition, in the future new materials may also be applied as FRP confinement.

For the case of *eccentrically loaded* FRP confined *circular* columns our aim is to develop a new model (Figure 1b) with the aid of which we wish to predict the experimental data and to explain the behavior of confined columns.

For *concentrically loaded* FRP confined *rectangular* columns our aim is to develop a model and design expressions for the calculation of failure loads.

3. METHOD OF SOLUTION

As we stated earlier simplified design-oriented models fail to properly predict the behavior of confined concrete. To fulfill our aim we will use an analysis-oriented model based on a sophisticated material law [5]. The following steps are performed:

- a finite element model is developed;
- the model is verified with available experimental data;
- several numerical calculations are performed by changing the geometrical and material properties of the confined column;
- empirical design expressions are developed by fitting curves on the results of the FE calculations.

4. MODEL

Material laws: The FRP confinement is modeled with the classical laminate plate theory and it is assumed that it behaves in a linearly elastic manner until failure. For the steel reinforcement – if present – a simple elastic-plastic stress-strain curve is used. For the concrete a new, quite accurate (confinement-sensitive, non-associated) material law is used proposed by Papanikolaou and Kappos [5]. Typical stress-strain diagrams are shown in Figure 5.

In Figure 5c for unconfined concrete after reaching the failure state the concrete softens and a decreasing path appears in the stress-strain diagram (solid line). This post-failure behavior changes due to the FRP confinement (dotted lines) and hence the confined concrete strength (f_{cc}) is higher than the unconfined concrete strength (f_{c0}). (*New results: 1.*)

This material law does not contain the time-dependent behavior of concrete, effects of creep and shrinkage are not investigated in this work.

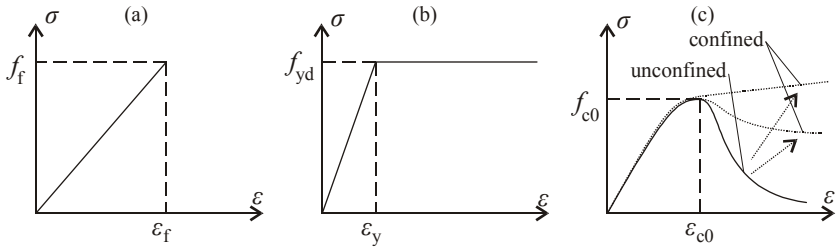

Figure 5: Typical stress-strain diagrams for the materials used in the model: FRP confinement (a), steel (b) and concrete (c).

Numerical model: A 2D finite element model was developed for the calculation of the cross-section (Figure 6). Note that the finite element mesh is two-dimensional, however the strains and stresses are three-dimensional: it is assumed that the axial strain varies linearly through the cross-section (and the nonlinearly varying axial stress is calculated by the FE code).

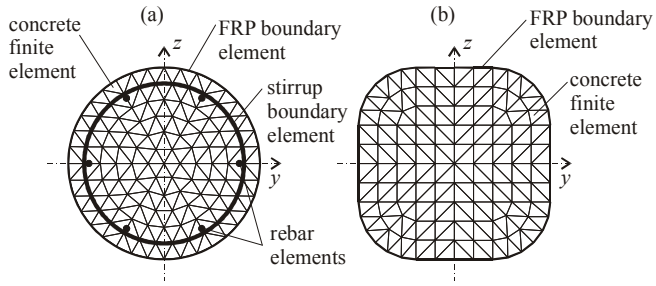

Figure 6: The finite element mesh of a circular cross-section with reinforcement (a) and rectangular cross-section (b).

Due to the high nonlinearity of the concrete material law a strain-controlled incremental calculation was implemented, the block diagram is shown in Figure 7. (*New results: 4., 5.*)

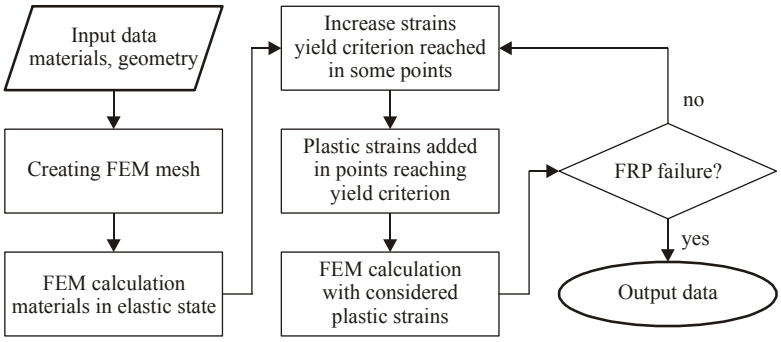

Figure 7: Block diagram of the calculation.

5. VERIFICATION

5.1 Concentrically loaded circular cross-sections

The axial concrete strengths at failure were calculated numerically for all the experimental cases (154 cases) and the average absolute error was found to be 9.95%. A few experimental stress-strain diagrams were compared with the calculations recommended by different authors and also with our model (Figure 8). It can be observed that the proposed model can follow the shape of the diagram, however the accuracy is poor because of the lack of material properties needed for the calibration of the concrete behavior.

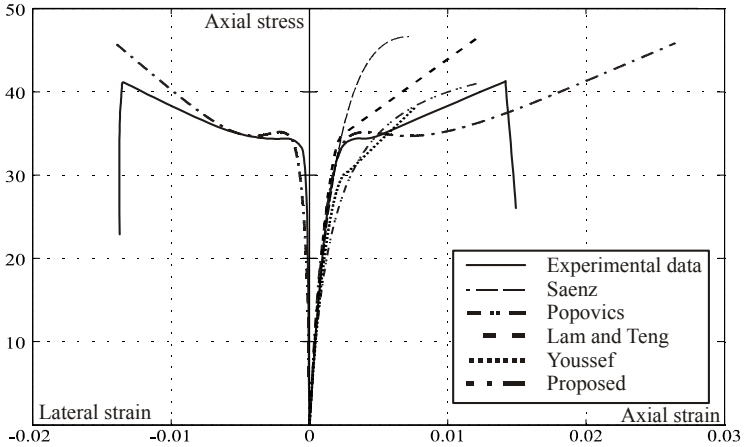

Figure 8: Comparison of the experimental results and the calculated $\sigma(\varepsilon)$ diagrams.

5.2 Eccentrically loaded circular cross-sections

The comparison of experimental results and numerical calculations is shown in Figure 9.

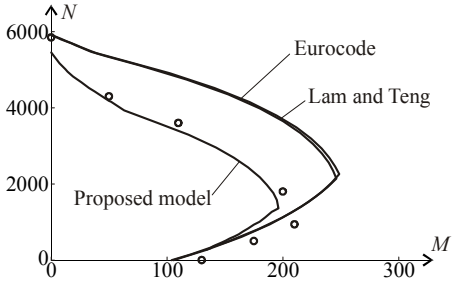

Figure 9: Comparison of experimental results found in the literature and models.

Our experiments: Fifteen circular column specimens were prepared and tested in our experimental program running in 2006 at the Budapest University of Technology and Economics. Six columns were confined with carbon fibers confined polymer (CFRP) and six were confined using glass fibers (GFRP). The remaining columns were used as control specimens. The instrumentation for a CFRP confined specimen can be seen in Figure 10.

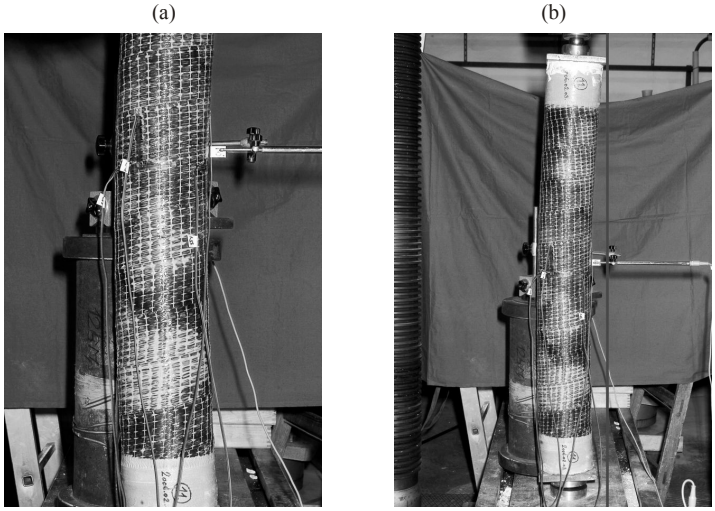

Figure 10: Instrumentation of specimen 11 (a) and the specimen curved due to the load (b).

Comparison of the load paths and the calculated capacity diagrams for GFRP confined columns are shown in Figure 11. For the calculation of the diagrams the measured maximal hoop strain was used instead of the rupture strain of the confining FRP. After the experiments the columns were cut and no delamination between the concrete core and the confining FRP was found.

Unfortunately, the experimental results of CFRP confined columns showed a very bad correlation with the calculated values. The reason can be the extremely poor quality of the manufactured concrete columns.

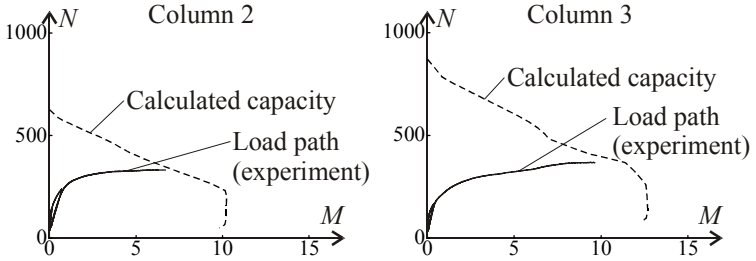

Figure 11: Comparison of the calculated load paths and the calculated capacity diagrams for GFRP confined columns.

5.3 Concentrically loaded rectangular cross-sections

For verifications first the experimental data of Wang and Wu [6] were compared with our numerical calculations (Figure 12).

Our experimental results are quite accurate, especially if the case of the unconfined circular cross-section was used for the determination of the concrete material properties (identified as "calibrated" results). We emphasize that our model is the only one (see Figure 4) which can predict the concave shape of the experimental data (*New results: 5.1.*).

We also calculated – without any calibration – the f_{cc} values for all available experiments, the average absolute error is 16.33%.

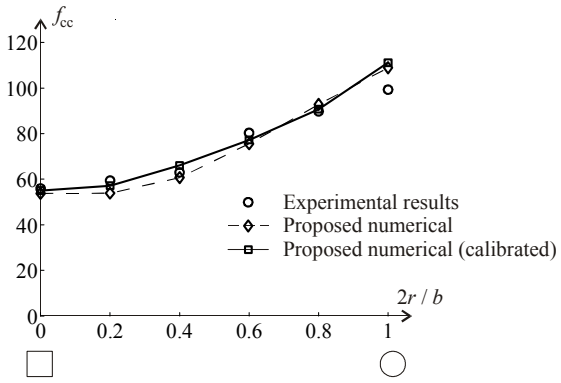

Figure 12: Comparison of experimental results with our models.

6. ACHIEVEMENTS

6.1 Concentrically loaded circular cross-sections

With the aid of the developed model we investigated the effect of the stiffness of the confinement. An example can be seen in Figure 13 for a C30 concrete with unidirectional confinement. Each solid line belongs to a given stiffness ratio (ρ_s) defined as (*New results: 1.*):

$$\rho_s = \frac{2E_f t}{dE_c}, \tag{2}$$

where E_c is the elastic modulus of concrete. (*New results: 1.*)

We may observe (Figure 13) that for higher stiffness the stress-strain curve is monotonic (curve c), while for lower stiffness the diagram has one local maximum point and one local minimum point (curve d). The rupture of confinement (and hence the concrete strength at failure) depends on the confinement ratio (ρ_c) [4].

$$\rho_c = f_l / f_{c0}, \tag{3}$$

In Figure 13 it can be seen that the stiffness affects the strength of the confined concrete (*New results: 1.*). Eight stress-strain diagrams are shown, which belong to different stiffnesses, however to the same strength (confinement ratio). The dots show the end of the stress-strain curves.

When the stiffness is very high the FRP ruptures before the concrete can reach the failure state (curve a, E_f = 765 kN/mm^2). This is defined as "overstiffened" concrete, and must be avoided (*New results: 1.2.*).

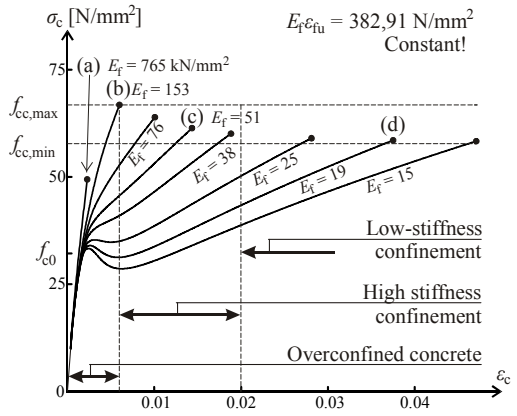

Figure 13: Effect of the stiffness of confinement on the stress-strain diagram of C30 concrete.

An "optimal stiffness" ($\rho_{s,opt}$) for the confinement can be found where the failure strength is maximum (curve b in Figure 13). This is also the limit between the overstiffened concrete and the high-stiffness confinement. The following curve was fitted on the numerically calculated results (*New results: 2.1.*):

$$\rho_{s,opt} = -0.1 + 0.22\rho_c^{0.2}\left(\frac{f_{c0}}{20}\right)^{0.3}. \tag{4}$$

If the stiffness is high (but lower than $\rho_{s,opt}$) higher failure strength can be achieved than for lower stiffness. The limit between high-stiffness and low-stiffness confinement was investigated numerically. The data can be approximated by the following expression (*New results: 2.1.*):

$$\rho_{s,limit} = \begin{cases} 0.0195 + \dfrac{f_{c0} - 40}{3100}, & \text{if } f_{c0} \le 40 \\ 0.0195 + \dfrac{f_{c0} - 40}{12000}, & \text{if } f_{c0} > 40 \end{cases}. \tag{5}$$

A simplified model is introduced where for low-stiffness confinement the following expression is *derived* from the model (*New results: 2.3.*):

$$f_{\mathrm{cc}} = \max \begin{Bmatrix} f_{\mathrm{cc,min}} \\ f_{\mathrm{c0}} \end{Bmatrix}, \tag{6}$$

for high-stiffness confinement the following approximation can be used (*New results: 2.3.*):

$$f_{\mathrm{cc}} = f_{\mathrm{cc,min}} + \left(f_{\mathrm{cc,max}} - f_{\mathrm{cc,min}} \right) \frac{\rho_{\mathrm{s}} - \rho_{\mathrm{s,limit}}}{\rho_{\mathrm{s,opt}} - \rho_{\mathrm{s,limit}}}, \tag{7}$$

where the limit values *derived* from the concrete material law are (*New results: 2.2.*):

$$f_{\mathrm{cc,min}} = f_l + \sqrt{10.16 f_l f_{\mathrm{c0}}}, \tag{8a}$$

$$f_{\mathrm{cc,max}} = f_l + \sqrt{10.16 f_l f_{\mathrm{c0}} + f_{\mathrm{c0}}^2}. \tag{8b}$$

The simplified method described above was compared with the experimental results found in the literature and 11.72% average absolute error was found.

6.2 Eccentrically loaded circular cross-sections

A typical calculated capacity diagram is shown in Figure 14 where the average axial stresses at failure in certain points are also indicated. The average axial stress decreases rapidly as we move away from the most compressed part of the cross-section, much faster than it is predicted by the models [1,2] based on the (linear) stress-strain diagram of Lam and Teng [4] recommended for concentrically loaded circular columns (*New results: 4.1.*).

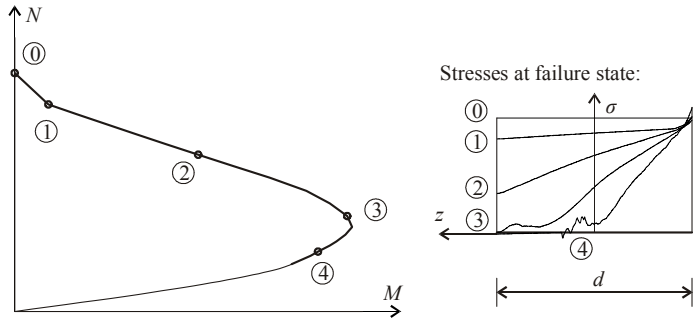

Figure 14: Average stress curves at failure.

Based on the average axial stresses simplified stress-strain diagrams (P1 or P2) are recommended as shown in Figure 15 (*New results: 4.2.*).

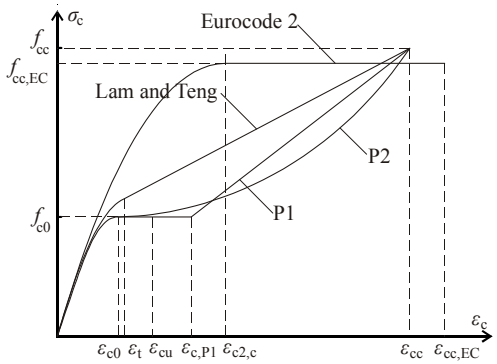

Figure 15: Stress-strain diagrams for simplified design.

We have calculated the capacity curves of experimental data available in the literature, and it was found that the Eurocode 2 [2] and the Lam and Teng [4] curves overestimate the failure load for eccentric loading, while both P1 and P2 seems reasonable (Figure 16).

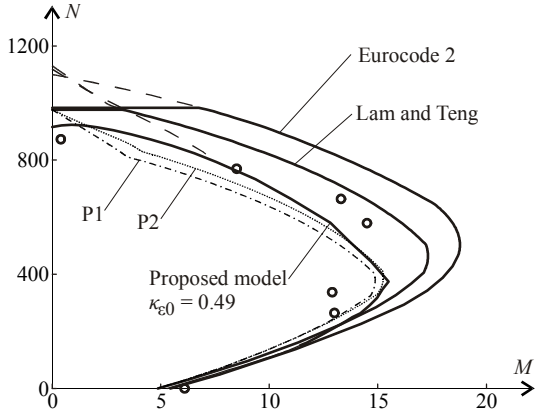

Figure 16: Capacity diagrams for simplified design (Bisby and Ranger).

6.3 Concentrically loaded rectangular cross-sections

According to the FE model two typical stress results are shown in Figure 16. The axial stresses are highest at the rounded edges and lowest (even zero) at the sides of the cross-section (*New results: 5.1.*).

The stresses within the cross-section are more complex than it is indicated by the simple division of the section into a confined and an unconfined area (as recommended by all simplified models). Therefore we decided to use the f_{cc} calculated for a circular confined column (with $d = b$, denoted by $f_{cc\circ}$) as a basis of the simplified method. Only square cross sections ($b = h$) with rounded edges are considered where the value of $f_{cc\circ}$ can be calculated using Equations (6 and 7) by assuming that $d = b$.

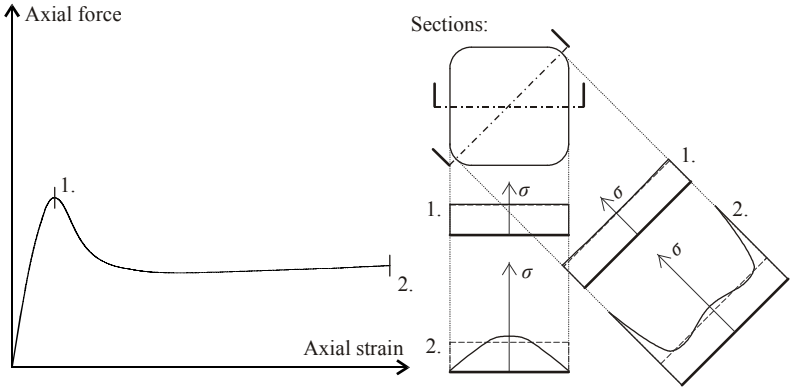

Figure 20: Axial stresses in rectangular cross-sections (f_{c0} is indicated by dashed lines).

The average axial strength (f_{cc}) of square sections with rounded edges are approximated as follows: For low-stiffness confinement ($\rho_{s\circ} \leq \rho_{s,limit}$):

$$f_{cc} = f_{cco}\left(1-\left(1-\left(\frac{2r}{b}\right)^2\right)\left(1-\frac{7.23}{\left(\frac{f_l}{f_{c0}}+2.22\right)^3}\right)-29.68\frac{f_l}{f_{c0}}\left(\rho_{s,limit}-\rho_{so}\right)\right), \quad (9)$$

(According to the results of the numerical calculations with high relative corner radius ($1 > 2r / b > 0.9$) a sudden drop appears in the value of f_{cc}. Due to this phenomenon the above presented equation underestimates the value of f_{cc} in case of circular cross-sections.)

For high-stiffness confinement ($\rho_{s\circ} > \rho_{s,limit}$):

$$f_{cc} = f_{cco}\left(1-\left(1-\left(\frac{2r}{b}\right)^2\right)\left(1-\left(\frac{7.23}{\left(\frac{f_l}{f_{c0}}+2.22\right)^3}\right)^{\left(\frac{\rho_{s,limit}+0.1061}{\rho_{so}+0.1061}\right)}\right)\right). \qquad (10)$$

(Note that the lower limit for both expressions is f_{c0}.)

The simplified expression was verified against the experimental results for square sections with rounded edges found in the literature. 13.18% average absolute error was found (*New results: 6.*).

7. NEW RESULTS

1. A new model is developed – based on a confinement-sensitive plasticity constitutive concrete material law – for the calculation of *concentrically loaded* FRP confined *circular* cross-sections. (Models found in the literature are built on less accurate concrete material laws.) The model was verified by comparing the results of the new numerical method with the experimental data found in the literature [7].
   Based on the model the following statements can be made:
   1.1. Contrary to the statements found in the literature the axial strength of the confined column depends on the stiffness of the confining FRP but this effect is negligible in case of "low-stiffness" confinement [7].
   1.2. It was found that "overstiffening" of the confinement is possible which leads to significantly lower axial strength than in case of low- or high-stiffness confinement [7].
   1.3. It was found that an "optimal stiffness" for the confinement can be defined which (for a given confinement ratio) leads to the maximal axial strength [7].
2. New expressions are recommended for *concentrically loaded* FRP confined *circular* concrete cross-sections [7]:
   2.1. Based on the results of numerical calculations simplified expressions are recommended for the calculation of low-, high-stiffness and optimal confinement and for the calculation of "overstiffening" [7].
   2.2. Based on the model new analytical expressions were *derived* to determine the strength of confined concrete in case of low-stiffness and optimal confinement (average error < 15%) [7].
   2.3. Based on the model simplified expressions are recommended for the calculation of axial strength in case of high-stiffness confinement (average error < 15%) [9].

3. By investigating the material properties of commonly used materials, it was found that if glass fibers are used the confinement is low-stiffness; while with carbon fibers high-stiffness confinement can be achieved [7].

4. A new model is presented – based on the Bernoulli-Navier hypothesis – for the calculation of *eccentrically loaded* FRP confined *circular* cross-sections. (Models based on concrete material laws for triaxial compression – that give qualitative results – can not be found in the literature.) The model was verified by comparing the results of the new numerical method with the experimental data found in the literature [8,9].
   Based on the model the following statements can be made:
   4.1. It was found that the axial resistance in case of high eccentricities can be significantly lower than predicted by the models found in the literature [8]. (Experimental results also verify this statement.)
   4.2. New stress-strain curves were recommended for a simple "design-oriented" model for the calculation of the capacity diagram of eccentrically loaded FRP confined circular cross-sections [8].

5. The model presented above was applied for the calculation of *concentrically loaded* FRP confined *rectangular* cross-sections. (Models found in literature are less sophisticated or built on less accurate concrete material laws.) The model was verified by comparing the results of the new numerical method with the experimental data found in the literature [10].
   Based on the model the following statements can be made:
   5.1. The exact axial stress-distribution in the cross-section was calculated [10]. (Only approximate methods were found in the literature.)
   5.2. The effect of the rounding of the edges on the axial strength was calculated [10]. (Models found in the literature did not give reliable results.)
   5.3. A new, simplified expression was recommended for the calculation of *concentrically loaded* FRP confined *rectangular* cross-sections. The accuracy of the new model is acceptable (<15%) [10].

REFERENCES

Referred articles

[1] Bisby, L. and Ranger, M., "Axial-flexural interaction in circular FRP-confined reinforced concrete columns", *Construction and Building Materials*, 24, 1672-1681 (2010).

[2] Eurocode 2: "Design of Concrete Structures – Part 1-1: General rules and rules for buildings", *ENV 1992-1-1*, (2003).

[3] Kármán, T., "Mitől függ az anyag igénybevétele?", *Magyar Mérnök- és Építész Egylet Közlönye*, 44(10), 212-226 (1910).

[4] Lam, L. and Teng, J. G., "Design-oriented stress-strain model for FRP-confined concrete", *Construction and Building Materials*, 17, 471-489 (2003).

[5] Papanikolaou, V. K. and Kappos, A. J., "Confinement-sensitive plasticity constitutive model for concrete in triaxial compression", *International Journal of Solids and Structures*, 44, 7021-7048 (2007).

[6] Wang, L-M. and Wu, Y-F., "Effect of corner radius on the performance of CFRP-confined square concrete columns: Test", *Engineering Structures*, 30, 493-505 (2008).

Publications

[7] Csuka, B. and Kollár, L. P., "FRP confined circular columns subjected to concentric loading", *Journal of Reinforced Plastics and Composites*, 29(23), 3504-3520 (2011).

[8] Csuka, B. and Kollár, L. P., "FRP confined circular columns subjected to eccentric loading", *Journal of Reinforced Plastics and Composites*, (article in press 2011).

[9] Csuka, B. and Kollár, L.P., "Analysis of FRP confined columns under eccentric loading", *Composite Structures*, (accepted for publication, 2011).

[10] Csuka, B. and Kollár, L. P., "FRP confined rectangular columns subjected to concentric loading", (Manuscript to be published at *Journal of Reinforced Plastics and Composites*).